Cerebrovascular
Diseases Extra

Cerebrovasc Dis Extra , DOI: 10.1159/000538548
Received: February 2, 2024
Accepted: March 24, 2024
Published online: March 28, 2024

Waveform Analysis of STA-MCA Bypass graft in Revascularization Surgery for Moyamoya Disease

Kochi R, Kanoke A, Tashiro R, Uchida H, Endo H

ISSN: (Print), eISSN: 1664-5456 (Online)
https://www.karger.com/CEE
Cerebrovascular Diseases Extra

Research Article

Waveform Analysis of STA-MCA Bypass graft in Revascularization Surgery for Moyamoya Disease

Ryuzaburo Kochi[a], Atsushi Kanoke[a], Ryosuke Tashiro[b], Hiroki Uchida[a], Hidenori Endo[b]

[a] Department of Neurosurgery, Kohnan Hospital, Sendai, Miyagi, Japan
[b] Department of Neurosurgery, Tohoku University Graduate School of Medicine, Sendai, Miyagi, Japan

Short Title: Waveform analysis of bypass surgery in Moyamoya disease

Corresponding Author:
Hidenori Endo M.D., Ph.D.
Department of Neurosurgery, Tohoku University Graduate School of Medicine
1-1 Seiryo-machi, Aoba-ku, Sendai, Miyagi 980-8574, Japan
Tel: +81-22-717-7230; Fax: +81-22-717-7233; E-mail: h-endo@nsg.med.tohoku.ac.jp

Number of Tables: 0
Number of Figures: 4 + sup
Word count: Abstract 257/Body text 1922

Keywords: Moyamoya disease, Bypass surgery, Cerebral Blood flow, Waveform, Hyperperfusion

Abstract
Introduction: Postoperative hyperperfusion syndrome (PHS) is a well-known complication following superficial temporal artery (STA)-middle cerebral artery (MCA) bypass for moyamoya disease (MMD). The early detection of postoperative radiological hyperperfusion (PRH), characterized by a transient increase in local cerebral blood flow (CBF), is crucial for the early diagnosis of PHS. This study aimed to investigate the effectiveness of waveform analysis for early PRH detection.
Methods: We reviewed 52 consecutive patients who underwent STA-MCA bypass for MMD. Patients were divided into PRH and non-PRH groups based on the postoperative/preoperative CBF ratio. We collected the intraoperative bypass graft waveform and bypass flow data using a flowmeter. The pulsatile index (PI), an indicator of peripheral vascular resistance (PVR), was calculated from bypass flow data. Next, the newly proposed index of PVR, the ratio of the time from peak to 50% decay and to 100% decay (RT50), was calculated through waveform analysis. The values were then compared between the PRH and non-PRH groups.
Results: Twenty-seven of the 52 patients met the inclusion criteria. Fourteen of these 27 patients showed PRH. The RT50, but not the PI, was significantly higher in the PRH group. Linear regression analysis revealed a significant correlation between the RT50 and PI. In the receiver operating characteristic for predicting PRH, the area under the curve of RT50 was 0.750, with a cutoff value of 0.255, a sensitivity of 0.928, and a specificity of 0.500.
Conclusion: The RT50 obtained from waveform analysis is associated with PVR and can be useful for the early detection of PRH in patients with MMD.

Introduction

Superficial temporal artery (STA)-middle cerebral artery (MCA) bypass is an effective revascularization technique to prevent future strokes in moyamoya disease (MMD) [1-5]. Postoperative hyperperfusion syndrome (PHS) is a well-known postoperative complication that can cause transient focal neurological deficits, vasogenic edema, and delayed intracranial hemorrhage [6-9]. PHS remains a major clinical challenge in terms of the prescriptive factor of clinical outcomes after revascularization surgery. Postoperative radiological hyperperfusion (PRH), characterized by a focal increase in cerebral blood flow (CBF), is a useful predictor of PHS [6-9]. Appropriate blood pressure control is crucial in reducing the risk of PHS after the detection of PRH by postoperative single-photon emission computed tomography (SPECT) [7]. However, PHS can occur immediately after or even during surgery [9], necessitating an earlier detection method. Intraoperative measurement of bypass blood flow using a flowmeter is a potential alternative for earlier detection of PHS [10-12]. In addition to blood flow values, this device can provide waveforms containing information about peripheral vascular resistance (PVR) [13]. In MMD, chronic hypoperfusion induces vasodilation of the ischemic territories through the vascular autoregulatory system, leading to decreased PVR, one of the underlying mechanisms of PHS [9]. Therefore, we hypothesized that the measurement of PVR by intraoperative waveform analysis would be useful for the early detection of PRH.

Materials and Methods

Inclusion criteria of patients

We reviewed a consecutive series of 52 patients with MMD who underwent STA-MCA bypass and encephalo-duro-myo-synangiosis (EDMS) between January 2021 and March 2022. The inclusion criteria were as follows: 1) patients who underwent intraoperative blood flow measurement and 2) patients who were assessed by SPECT before and after surgery. The diagnosis of MMD followed the previous literature [14]. Surgical indication was decided on the basis of a comprehensive assessment, which considered the following: presence of ischemic symptoms or a history of posterior hemorrhage [15], evident hemodynamic compromise on SPECT, independent activities of daily living, and the absence of cerebral infarction that exceeded the vascular territory of a major branch of the MCA.

Surgical procedure

All patients underwent STA–MCA anastomosis with EDMS under general anesthesia by a single surgeon (H.E.). Craniotomy was performed around the sylvian fissure end. The stump of the STA, either the frontal or parietal branch, was anastomosed to the M4 segment of the MCA, followed by EDMS. The patency of the STA-MCA anastomosis was confirmed by intraoperative indocyanine green video angiography and Doppler ultrasonography [7, 16].

Intraoperative bypass flow measurement and waveform analysis

Intraoperative measurement of bypass flow was conducted using a flexible perivascular flow probe (HQN-1.5 MB-1.5 mm, HQN-2 MB-2.0 mm; Transonic Systems Inc., Ithaca, NY, USA) and a transit time flowmeter (HT353, Transonic System, Ithaca, NY, USA). This device provided quantitative blood flow data, including maximum flow (mL/min), minimum flow (mL/min), mean flow (mL/min), and a waveform of the bypass graft. Using these quantitative blood flow data, the pulsatile index (PI), an indicator of PVR, was calculated using the following equation [17]:

PI = (max flow − minimum flow) / (mean flow)

In addition, we performed original waveform analysis to assess PVR based on the idea that waveform changes reflect PVR [13]. The averaged blood flow waveform was obtained from 10-s measurements (MATLAB 2019a, The MathWorks Inc., Natick, MA, USA). A peak of the averaged waveform was set as the reference point of the time course. The ratio of the time from peak to 50% decay and to 100% decay (RT50) was calculated using the following equation:

RT50 = (Time from peak to 50% decay) / (Time from peak to 100% decay)

An example of RT50 calculated from the averaged waveform is displayed in Figure 1.

Radiological evaluation

Pre- and postoperative CBF was assessed using the autoradiographic method with ^{123}I-iodoamphetamine (IMP)-SPECT (Infinia Hawkeye 4; GE Healthcare, Tokyo, Japan) [18]. Preoperative CBF measurements were typically obtained within 2 months prior to surgery. We quantitatively measured the CBF by manual definition of a region of interest (ROI) with a diameter of 1 cm at the exact vascular territory supplied by the bypass and the ipsilateral cerebellum [18]. The exact vascular territory supplied by the bypass was determined by comparing the original axial slice on postoperative magnetic resonance arthrography (MRA) and ^{123}I-IMP SPECT. Both the pre- and postoperative CBF values were adjusted by the CBF value of the ipsilateral cerebellar hemisphere to calculate the postoperative/preoperative CBF ratio within the ROI [18]. PRH was defined as a greater than 120% increase in the postoperative/preoperative CBF ratio. Although the definition of RHP varies among previous studies [7-9, 19], we defined the threshold of RHP as 120% increase to detcect mild hyperperfusion.

Statistical analysis

We performed a comparative analysis between the non-PRH and PRH groups using the RT50, PI, maximum flow, mean flow, minimum flow, preoperative CBF, temporary occlusion time, diameter of recipient artery, and diameter of STA, which are reported potential risk factors for PHS [10-12. 20-22]. The Wilcoxon rank-sum test or Peason's chi-square test was applied for the comparisons between the two groups, and a linear regression analysis was conducted to examine the relationship between the postoperative/preoperative CBF ratio and the aforementioned parameters. Receiver operating characteristic (ROC) analysis was used to assess the accuracy of the RT50 and preoperative normalized CBF for the detection of PRH [9. 23]. Statistical analyses were performed using JMP Pro 12 (SAS Institute, North Carolina, USA), and significance was defined at a p-value of 0.05.

Results

Twenty-seven patients met the inclusion criteria. Fourteen (52%) of the 27 patients exhibited PRH; the median age at surgery was 42 (range: 17–66), 11 (79%) patients were female, 6 (43%) had left-side surgery, 2 (14%) had hemorrhagic onset, and 12 (86%) had ischemic onset. The clinical backgrounds of the 13 patients in the non-PRH group were as follows: the median age was 35 years (range: 24–65), 10 (77%) patients were female, 5 (38%) had left-side surgery, 4 (31%) had hemorrhage onset, and 8 (62%) had ischemic onset. There were no statistical differences in these background factors between the two groups. Four out of 27 patients (15%) developed PHS, and all of them were included in the PRH group (31%). In four patients with PHS, one patient had intracerebral hemorrhage and the other three manifested transient neurological deficits. None of these events affected the clinical outcomes.

Next, we compared the intraoperative and neuroradiological data between the PRH and non-PRH groups (Figure 2, a–i). Among the variables compared, only the RT50 was significantly different between the two groups; the PRH group demonstrated a higher RT50 than the non-PRH group (p = 0.047) (Fig. 2a). In the linear regression analysis investigating the correlation between the RT50 and other variables, a significant correlation was found only between PI and RT50 ($y = 1.26–1.68x$, R-square: 0.35, p = 0.001) (Supplementary Figure). In the ROC analysis to predict PRH, the area under the curve (AUC) of RT50 was 0.750, with a cutoff value of 0.255, a sensitivity of 0.928, and a specificity of 0.500, whereas the AUC of preoperative CBF was 0.565, with a cutoff value of 0.644, a sensitivity of 0.29, and a specificity of 0.00 (Figure 3).

Representative case

A 45-year-old male presented with transient left upper limb weakness and was diagnosed with MMD through neuroradiological assessment, including digital subtraction angiography, which revealed Suzuki stage 3 MMD in the right hemisphere (Fig. 4a). MRI revealed scattered old infarctions, and SPECT showed a significant CBF decrease in the right MCA area (not shown). Because the patient was diagnosed with symptomatic MMD with impaired cerebral hemodynamics, we performed STA-MCA anastomosis in the right hemisphere (Fig. 4b). Intraoperative flowmeter analysis for the STA graft showed a maximum flow of 165.7 mL/s, a mean flow of 118.8 mL/s, a minimum flow of 85.0 mL/s, a PI of 0.68, and an RT50 of 0.27 (Fig. 1a). The patient was awake after surgery without any neurological deterioration. Postoperative MRA showed good patency of the bypass graft (Fig. 4c). SPECT the day after surgery revealed a 233.9% CBF increase at the site of anastomosis, indicating RHP (Fig. 4d, right). Based on the results of waveform analysis and SPECT, we managed this patient with strict blood pressure control to prevent the development of HPS. The patient remained symptom-free and was discharged 8 days after surgery. Figure 1a is averaged waveform of this patinet, and figure 1b is averaged waveform of a non-RHP patient (RT50: 0.14, 113.4% CBF increase).

Discussion

This study is the first to demonstrate the utility of waveform analysis of the bypass graft for predicting PRH in MMD. The RT50, the original value calculated from the waveform analysis as the index for PVR, was found to be significantly higher in the PRH group. ROC analysis showed that the RT50 can be a more useful factor than preoperative CBF status for predicting PRH.

A blood flow wave is observed as the sum of a forward wave from the heart and a backward reflected wave. In general, the amplitude and speed of the backward wave are positively correlated with impedance, such as PVR, and the backward wave causes flow to change in the opposite direction [13]. Hence, the amplitude and speed of the backward wave become lower and slower under the condition of decreasing PVR. Consequently, the amplitude of the observed flow wave rises, and the downhill slope of the observed wave is gradual, increasing the RT50. The PI can be used to evaluate the PVR, and an increased PI can indicate an increased PVR in the distal vascular territories [17]. We confirmed a strong negative correlation between RT50 and PI, which suggests that a higher RT50 indicates decreased PVR. Therefore, the higher RT50 in the PRH group was thought to reflect decreased PVR in the PRH group compared with that in the non-PRH group. In contrast, there were no significant differences in PI between the two groups. It is important to note that factors such as age and sex can influence the PI [24], affecting the results of this study.

Contrary to previous reports, there were no significant differences in blood flow value, preoperative CBF, and diameter of the bypass graft between the two groups in our study. Differences in sample size, timing of SPECT, definition of PRH, and surgical methodology are plausible reasons for this. Blood flow values are easily influenced by factors such as blood pressure, cardiac output, and diameter of the bypass graft. In contrast, waveform analysis is less susceptible to these factors because both forward and backward waves are equally affected, canceling out the influence of these factors.

One of the limitations of this study is the small sample size collected in a single center. This may have affected the non-significant correlation between the RT50 and the postoperative/preoperative CBF ratio (Supplementary Figure), whereas the RT50 was significantly higher in the PRH group. The limited sample size also prevented reliable multivariate analysis, emphasizing the necessity for further investigations with larger cohorts. Moreover, we did not compare the waveform analysis and cerebrovascular reserve capacity (CVR), which are also associated with PVR [25]. The ROC analysis of the RT50, which indicated high sensitivity and low specificity, facilitates the creation of multimodal models, including waveform analysis and CVR, in the future.

Conclusion

Waveform analysis is a noninvasive and real-time tool that can be useful for the early detection of PRH in patients with MMD.

Statement of Ethics

The present study conforms to the guidelines issued in the Declaration of Helsinki. This study was approved by the Ethics Committees of Kohnan Hospital (approval number: 2020-0520-03). Written informed consent was obtained from all the participants. We have also received written informed consent for the publication of identifying details and accompanying images for representative case.

Conflict of Interest Statement

The authors have no conflicts of interest to declare.

Funding Sources

JSPS KAKENHI Grant No. 23K08491 supported English proofreading fee.

Author Contributions

R.K. and H.E.: conception and design. R.K., H.E., R.T., A.K, and H.U: acquisition of data. . R.K., H.E., and R.T.: analysis and interpretation. R.K.: drafting. H.E.: critical revision of the article. H.E.: study supervision.

Data Availability Statement

The data that support the findings of this study are not publicly available due to their containing information that could compromise the privacy of research participants. Further enquiries can be directed to the corresponding author.

References

1. Ishikawa T, Houkin K, Kamiyama H, Abe H. Effects of surgical revascularization on outcome of patients with pediatric moyamoya disease. Stroke. 1997 Jun;28(6):1170–1173.
2. Karasawa J, Touho H, Ohnishi H, Miyamoto S, Kikuchi H. Long-term follow-up study after extracranial–intracranial bypass surgery for anterior circulation ischemia in childhood moyamoya disease. J Neurosurg. 1992 July;77(1):84–89.
3. Miyamoto S, Akiyama Y, Nagata I, Karasawa J, Nozaki K, Hashimoto N, et al. Long-term outcome after STA-MCA anastomosis for moyamoya disease. Neurosurg Focus. 1998;5(5):7.
4. Guzman R, Lee M, Achrol A, Bell-Stephens T, Kelly M, Do HM, et al. Clinical outcome after 450 revascularization procedures for moyamoya disease. Clinical article. J Neurosurg. 2009 Nov;111(5):927–935.
5. Kuroda S, Houkin K, Ishikawa T, Nakayama N, Iwasaki Y. Novel bypass surgery for moyamoya disease using pericranial flap: its impacts on cerebral hemodynamics and long-term outcome. Neurosurgery. 2010 June;66(6):1093–1101.
6. Hayashi K, Horie N, Suyama K, Nagata I. Incidence and clinical feature of symptomatic cerebral hyperperfusion syndrome following vascular reconstruction. World Neurosurg. 2011 Nov;78(5):447-454.
7. Fujimura M, Shimizu H, Inoue T, Mugikura S, Saito A, Tominaga T. Significance of focal cerebral hyperperfusion as a cause of transient neurologic deterioration after extracranial- intracranial bypass for moyamoya disease: comparative study with non-moyamoya patients using N-isopropyl-p-[(123)I]iodoamphetamine single-photon emission computed tomography. Neurosurgery. 2011 Apr;68(4):957–64.
8. Fujimura M, Mugikura S, Kaneta T, Shimizu H, Tominaga T. Incidence and risk factors for symptomatic cerebral hyperperfusion after superficial temporal artery-middle cerebral artery anastomosis in patients with Moyamoya disease. Surg Neurol. 2009 Apr;71(4):442–7.
9. Uchino H, Kuroda S, Hirata K, Shiga T, Houkin K, Tamaki N. Predictors and clinical features of postoperative hyperperfusion after surgical revascularization for moyamoya disease: a serial single photon emission CT/positron emission tomography study. Stroke.
2012 Oct; 43(10):2610–6.
10. Nakamura A, Kawashima A, Nomura S, Kawamata T. Measurement of Intraoperative Graft Flow Predicts Radiological Hyperperfusion during Bypass Surgery in Patients with Moyamoya Disease. Cerebrovascular Diseases Extra. 2020 Jul;10(2):66-75.
11. Nakayama N, Kuroda S, Houkin K, Takikawa S, Abe H. Intraoperative measurement of arterial blood flow using a transit time flowmeter: monitoring of hemodynamic changes during cerebrovascular surgery. Acta neurochirurgica. 2001 Jan;143:17-24.
12. Lee M, Guzman R, Bell-Stephens T, Steinberg GK. Intraoperative blood flow analysis of direct revascularization procedures in patients with moyamoya disease. Journal of cerebral blood flow & metabolism. 2011 Jan;31(1):262-274.
13. Mynard JP, Kondiboyina A, Kowalski R, Cheung MM, Smolich JJ. Measurement, analysis and interpretation of pressure/flow waves in blood vessels. Frontiers in Physiology. 2020 Aug;11:1085.
14. Kuroda S, Fujimura M, Takahashi J, Kataoka H, Iwama T, Tominaga T, Miyamoto S. Revision 2021 of The Guideline for The Diagnosis of Moyamoya Disease by Research Committee on Moyamoya Disease (Spontaneous Occlusion of Circle of Willis). Surg Cereb Stroke. 2022;50:1-7
15. Takahashi JC, Funaki T, Houkin K, Inoue T, Ogasawara K, Nakagawara J, et al.; JAM Trial Investigators. Significance of the Hemorrhagic Site for Recurrent Bleeding: Prespecified Analysis in the Japan Adult Moyamoya Trial. Stroke. 2016 Jan; 47(1): 37–43.
16. Fujimura M, Tominaga T. Lessons learned from moyamoya disease: outcome of direct/indirect revascularization surgery for 150 affected hemispheres. Neurol Med Chir (Tokyo). 2012;52(5):327–32.
17. Harris S, Reyhan T, Ramli Y, Prihartono J, Kurniawan M. Middle cerebral artery pulsatility index as predictor of cognitive impairment in hypertensive patients. Frontiers in neurology. 2018 Jul;9:538.
18. Fujimura M, Niizuma K, Endo H, Sato K, Inoue T, Shimizu H, et al. Quantitative analysisof early postoperative cerebral blood flow contributes to the prediction and diagnosis of cerebral hyperperfusion syndrome after revascularization surgery for moyamoya disease.
Neurol Res. 2015 Feb;37(2):131–8.
19. Tashiro R, Fujimura M, Katsuki M, Nishizawa T, Tomata Y, Niizuma K, et al. Prolonged/delayed cerebral hyperperfusion in adult patients with moyamoya disease with RNF213 gene polymorphism c. 14576G> A

(rs112735431) after superficial temporal artery–middle cerebral artery anastomosis. Journal of Neurosurgery. 2020; 135(2), 417-424.

20. Horie N, Fukuda Y, Izumo T, Hayashi K, Suyama K, Nagata I. Indocyanine green videoangiography for assessment of postoperative hyperperfusion in moyamoya disease. Acta neurochirurgica. 2014;156:919-926.
21. Fujimura M, Niizuma K, Inoue T, Sato K, Endo H, Shimizu H, et al. Minocycline prevents focal neurological deterioration due to cerebral hyperperfusion after extracranial-intracranial bypass for moyamoya disease. Neurosurgery. 2014;74(2):163-170.
22. Uchida H, Endo H, Fujimura M, Endo T, Niizuma K, Tominaga T. Intra-operative hemorrhage due to hyperperfusion during direct revascularization surgery in an adult patient with moyamoya disease: a case report. Neurosurgical Review. 2017;40:679-684.
23. Yoshimoto T, Houkin K, Kuroda S, Abe H, Kashiwaba T. Low cerebral blood flow and perfusion reserve induce hyperperfusion after surgical revascularization: case reports and analysis of cerebral hemodynamics. Surgical neurology. 1997;48(2), 132-8.
24. Alwatban MR, Aaron SE, Kaufman CS, Barnes JN, Brassard P, Ward JL, et al. Effects of age and sex on middle cerebral artery blood velocity and flow pulsatility index across the adult lifespan. Journal of Applied Physiology. 2021;130(6):1675-1683.
25. Hirano T, Minematsu K, Hasegawa Y, Tanaka Y, Hayashida K, Yamaguchi T. Acetazolamide reactivity on 123I-IMP single photon emission computed tomography in patients with major cerebral artery occlusive disease: correlation with positron emission tomography parameters. Journal of Cerebral Blood Flow & Metabolism. 1994;14(5),763-770.

Figure legends

Fig. 1. Averaged waveform of blood flow. The ratio of time from peak to 50% decay and to 100% decay (RT50) was calculated as A/B. (a) Averaged waveform of RHP patient. (b) Averaged waveform of a non-RHP patient.

Fig. 2. Box-whisker plot of non-postoperative radiological hyperperfusion (PRH) and PRH by (a) RT50, (b) pulsatility index, (c) maximum flow, (d) mean flow, (e) minimum flow, (f) normalized preoperative cerebral blood flow (CBF), (g) temporary occlusion artery, (h) diameter of recipient artery, and (i) diameter of superficial temporal artery (STA). RT50: ratio of time from peak to 50% decay and to 100% decay.

Fig. 3. Receiver operating characteristic analysis for evaluating the performance of RT50 and normalized preoperative cerebral blood flow (pre-CBF) for the detection of radiological hyperperfusion.

Fig. 4. (a) Preoperative digital subtraction angiography of the right internal carotid artery (b) Intraoperative image of anastomosis of the right supratemporal artery (arrowhead) and right middle cerebral artery (M4) (arrow). (c) Postoperative magnetic resonance angiography 2 days after surgery demonstrated patency of the bypass artery (arrowhead). (d) Preoperative (left) and postoperative (right) single-photon emission computed tomography. Increased local cerebral blood flow was observed in the right frontal region where superficial temporal artery and middle cerebellar artery anastomosis was performed (arrowhead).

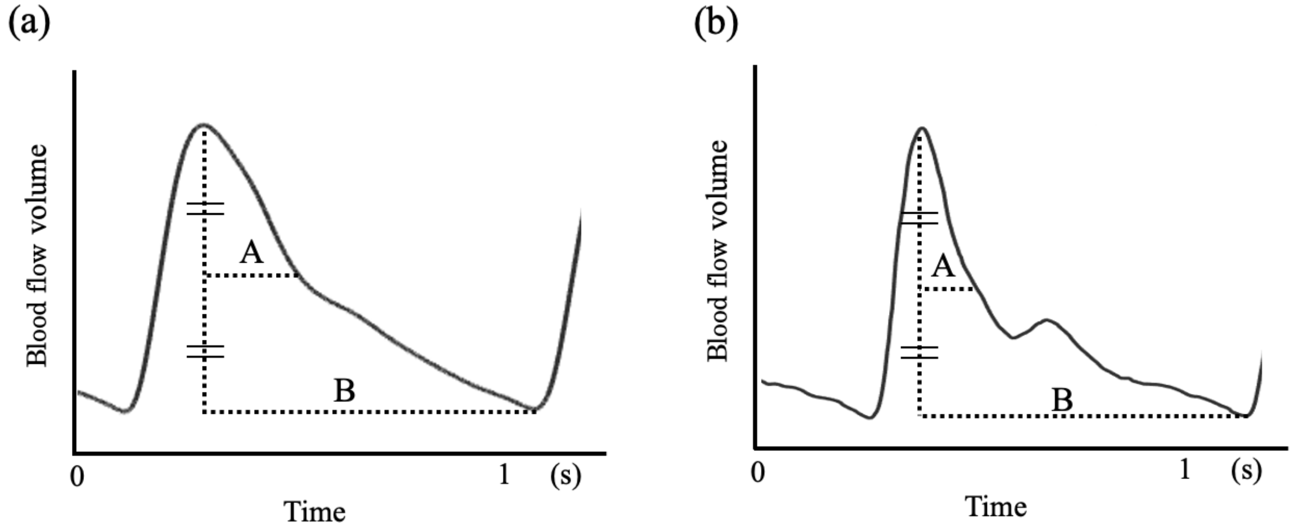
(a)
Blood flow volume
A
B
0
1
(s)
Time
(b)
Blood flow volume
A
B
0
1
(s)
Time

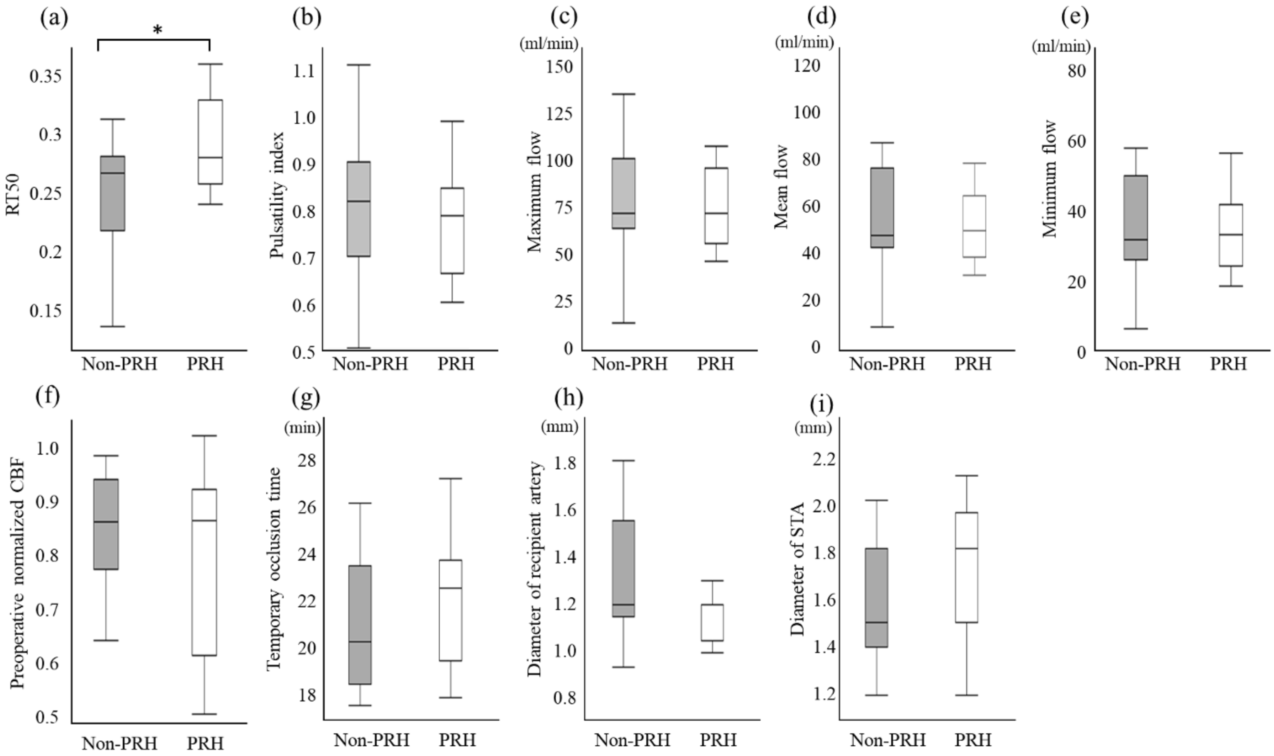
(a)
*
RT50
0.35
0.3
0.25
0.2
0.15
Non-PRH
PRH
(b)
Pulsatility index
1.1
1.0
0.9
0.8
0.7
0.6
0.5
Non-PRH
PRH
(c)
(ml/min)
Maximum flow
150
125
100
75
50
25
0
Non-PRH
PRH
(d)
(ml/min)
Mean flow
120
100
80
60
40
20
0
Non-PRH
PRH
(e)
(ml/min)
Minimum flow
80
60
40
20
0
Non-PRH
PRH
(f)
Preoperative normalized CBF
1.0
0.9
0.8
0.7
0.6
0.5
Non-PRH
PRH
(g)
(min)
Temporary occlusion time
28
26
24
22
20
18
Non-PRH
PRH
(h)
(mm)
Diameter of recipient artery
1.8
1.6
1.4
1.2
1.0
0.8
Non-PRH
PRH
(i)
(mm)
Diameter of STA
2.2
2.0
1.8
1.6
1.4
1.2
Non-PRH
PRH

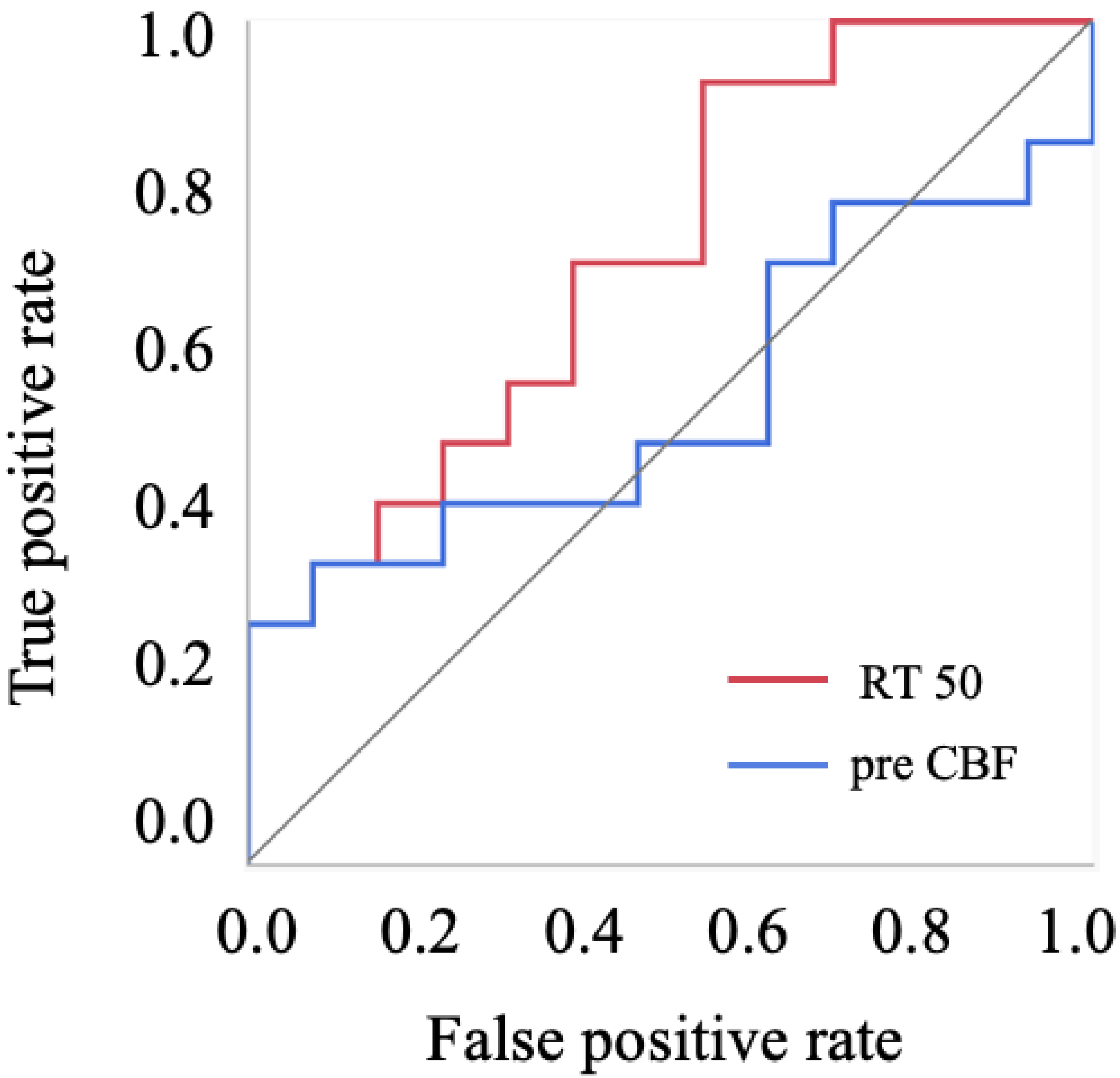
1.0
0.8
0.6
0.4
0.2
0.0
True positive rate
RT 50
pre CBF
0.0
0.2
0.4
0.6
0.8
1.0
False positive rate

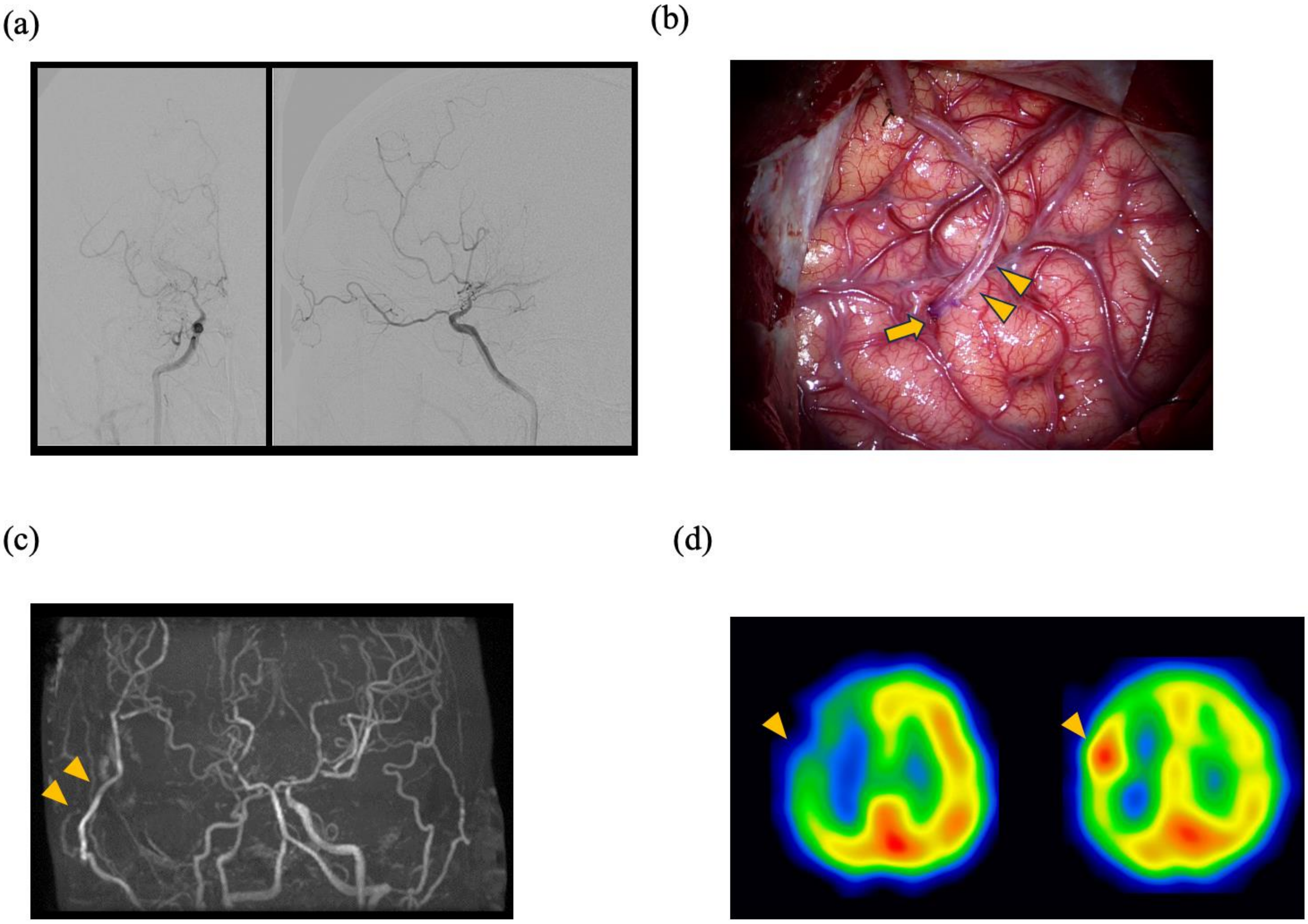
(a)
(b)
(c)
(d)